



# Assessment of Osteonecrosis in the Presence of Instrumentation for Femoral Neck Fracture Using Contrast-Enhanced MAVRIC Sequence

Nadja A. Farshad-Amacker, MD · Matthew F. Koff, PhD  · Jonathan P. Dyke, PhD · Lionel E. Lazaro, MD · Parina Shah, MS · Dean G. Lorich, MD · Hollis G. Potter, MD

Received: 1 July 2015/Accepted: 15 September 2015/Published online: 8 October 2015  
© Hospital for Special Surgery 2015

**Abstract** *Background:* Evaluating postoperative femoral neck fracture (FNF) with metal fixation hardware is commonly performed using radiographs. MRI has greater sensitivity and specificity to evaluate osteonecrosis (ON) but is often challenging due to the image distortion caused by metallic hardware. *Questions/Purposes:* The aim of this study is to compare fast spin-echo (FSE) and multi-acquisition variable-resonance image combination (MAVRIC) sequences in assessing ON following metallic fixation of FNF and determining feasibility of semi-quantitative perfusion using MAVRIC. *Methods:* Radiography and MRI were performed at 3 and 12 months postoperatively, using FSE and pre- and post-gadolinium contrast MAVRIC sequences in 21 FNF patients. The presence and volume of ON were recorded. Signal intensity (SI) enhancement was measured on the MAVRIC sequences within the

center and rim of ON; with the ilium and femoral diaphysis as controls. The detection rate of ON between MAVRIC and FSE images was evaluated as the difference of percent enhancement across the defined regions of interest. *Results:* ON was detected in 0% of radiographs, in 67% of FSE, and in 76% of MAVRIC images at 3 months follow-up, with similar results at 12 months. MAVRIC images had larger ON volume than FSE images at both time points. A significant percentage SI enhancement was only detected in the ON rim. *Conclusion:* Radiographs could not detect ON following metallic fixation of FNF. MAVRIC is more sensitive than FSE for determining the volume of ON. SI measurements using MAVRIC may provide an indirect assessment of perfusion.

**Keywords** osteonecrosis · avascular necrosis · femoral neck fracture · metal artifact

Level of Evidence: II: Development of diagnostic criteria on consecutive patients (with universally applied reference “gold” standard)

**Electronic supplementary material** The online version of this article (doi:10.1007/s11420-015-9475-3) contains supplementary material, which is available to authorized users.

N. A. Farshad-Amacker, MD · M. F. Koff, PhD (✉) · P. Shah, MS · H. G. Potter, MD  
MRI Research Laboratory, Hospital for Special Surgery,  
535 East 70th Street, BW-08G,  
New York, NY 10021, USA  
e-mail: koffm@hss.edu

J. P. Dyke, PhD  
Department of Radiology  
Weill Cornell Medical College,  
New York, NY 10065, USA

L. E. Lazaro, MD · D. G. Lorich, MD  
Department of Orthopedic Surgery, Hospital of Special Surgery,  
535 East 70th Street,  
New York, NY 10021, USA

## Introduction

Femoral neck fractures (FNF) are prevalent in patients with osteoporosis [11, 17, 26]. A complication of FNF is femoral head avascular necrosis/osteonecrosis (ON) and non-union, particularly in displaced FNF, attributed to femoral head ischemia [2, 7]. Although patients with ON after FNF fixation may remain asymptomatic, undiagnosed ON could cause unexplained and underreported pain after surgical fixation of the fracture [15]. The risk of collapse and eventual development of hip osteoarthritis emphasizes the clinical need of early detection and close follow-up with advanced imaging.

Most fracture complications are assessed by postoperative radiographs, which are limited by the two-dimensional imaging technique and poor soft tissue contrast. The prevalence of ON using radiographs is between 11 and 25% when using internal fixation after

FNF [4, 16, 18, 27, 28] and up to 40% following displaced fractures [29].

MRI is the most sensitive (99%), specific (99%) [25], and accurate non-invasive imaging modality [24] for early detection of ON, compared to radiography and scintigraphy [3, 33, 34]. A prior MRI study of FNF demonstrated an ON prevalence of 47%, with most patients presenting with non-displaced FNF [32]. A limitation of MRI following surgical fixation of FNF is magnetic susceptibility artifact, results in slice, and frequency misregistration of signal encoding. The artifact obscures visualization of soft tissue and osseous detail adjacent to the stainless steel instrumentation. Susceptibility artifact may be diminished by using a wide read-out bandwidth [14], but slice encoding distortions will still be present. Newer, three-dimensional (3D) multi-spectral imaging (MSI) techniques, such as the multi-acquisition variable-resonance image combination (MAVRIC) sequence, mitigate in-plane and through-plane metal susceptibility artifacts to allow detection of bone and soft tissue detail around metallic implants [13, 20, 21]. The prevalence of ON following metallic fixation of displaced FNF remains unclear using sequences with metal artifact reduction protocols. As MRI is considered the standard by which ON is diagnosed in hips without instrumentation, the same should apply following placement of instrumentation, and the newer 3D MSI techniques such as MAVRIC may facilitate diagnosis and aid in local perfusion measurements in the presence of instrumentation.

Therefore, the purposes of the study were (1) to compare the ability of two-dimensional (2D) fast spin-echo (FSE) and MAVRIC sequences to visualize ON around stainless steel instrumentation in FNF patients and (2) to determine the feasibility of performing estimated semi-quantitative perfusion measurements in the bone marrow with the MAVRIC sequence. We hypothesized that the prevalence of ON would be greater than that determined by traditional radiographic assessment alone.

## Patients and Methods

Institutional Review Board (IRB) approval with informed consent was obtained prior to data acquisition. The inclusion criteria for patients were (1) over 18 years of age, (2) presentation with sub-capital fracture of the femoral neck, and (3) normal kidney function as determined by glomerular filtration rate (GFR). Exclusion criteria were (1) prior allergic reaction to gadolinium contrast, (2) MR incompatibility with implanted ferromagnetic devices, (3) pregnancy, or (4) breast feeding. MR images of 21 consecutive patients (5 male, 16 female,  $61.7 \pm 12.2$  years [mean  $\pm$  SD]) were acquired immediately following FNF, at  $3.4 \pm 0.9$  months, and at  $12.0 \pm 0.6$  months after FNF repair. All repairs were performed with two stainless steel pin fixation (Synthese, West Chester, PA) and a fibular cortical bone

allograft placement. The right side was affected in 53% (11/21) of the patients and 95% (20/21) of patients had displaced FNF; Garden I:  $n=0$ , Garden II:  $n=1$ , Garden III:  $n=16$ , and Garden IV:  $n=4$  [8].

All MR imaging was performed with a 1.5-T clinical scanner system (450 DVMR, General Electric Health Care, Waukesha, WI) using eight-channel phased-array cardiac coil (GE Healthcare, Waukesha, WI). 2D -FSE proton density images were acquired in three orthogonal planes at all time points. Pre- and post-contrast MAVRIC images were obtained in the coronal plane at 3 and 12 months postoperatively. Imaging parameters are summarized in Table 1. Conventional radiographs were acquired in all patients preoperatively, immediately after FNF and at 3 and 12 months after surgery.

The presence of ON was recorded on conventional radiographs by radiologists blinded to the MRI results. The presence, location, and volume of ON were recorded using the 2D-FSE and MAVRIC sequence each at both time points (3 and 12 months after surgery) by two blinded, independent radiologists with 5 and 20 years of experience, respectively. ON was considered to be present when a double serpentine line representing the ischemic-viable bone interface was visible [25]. Solitary increased bone marrow signal intensity in absence of a double serpentine line was not considered to be ON [36]. The presence and location of the ON lesion was documented using picture archiving and communication system (PACS) (Sectra IDS7, version 12.5.0.234, Sweden). Volume measurements of the ON lesion seen across FSE and MAVRIC images were performed using OsiriX software (version 5.0.2) by two readers.

Post-contrast MAVRIC images were acquired after intravenous administration of 0.1 mol/kg Gadolinium-diethylenetriamine penta-acetic acid (Gd-DTPA, Magnevist<sup>®</sup>; Bayer HealthCare Pharmaceuticals Inc., Wayne, NJ) at a rate of 2 cc/s followed by a saline flush. The signal intensity (SI) was measured in pre- and post-contrast coronal MAVRIC images with regions of interest (ROIs) placed in the center of the ON, in the rim of the ON, in the marrow of the ilium, in the marrow of the femoral diaphysis (FD), and in the cortical bone of the femur (Fig. 1) by the same two independent radiologists. The pre- and post-contrast images were linked together to ensure that the placed ROIs were exactly the same size and at the exact same location on both images (Fig. 1). Standardized ROIs were set to  $19.8 \text{ mm}^2$  unless the anatomy was too small such that partial volume artifacts would affect the measurements.

The percent (%) SI enhancement was calculated as following:

$$\% \text{ Enhancement} = (B - A) / A$$

$A$  = SI without contrast in the ROI/SI without contrast in the ROI of cortical bone

$B$  = SI after contrast administration in the ROI/SI after contrast administration in the ROI of cortical bone

**Table 1** MR protocols

	2D-FSE PDw	MAVRIC
Repetition time	3500–4000 ms	1000
Echo time	23–28 ms	10–14 ms
Slice thickness	2.5–4 mm	3.5
Slice spacing	0 mm	0 mm
Number of excitations	3–5	0.5
Field of view	24–28 cm	38–44 cm
Echo train length	14–24	8
Receiver bandwidth	±125 kHz	±125 kHz
Receiver bandwidth	488 Hz/pixel	488 Hz/pixel
Acquisition matrix (frequency×phase)	512×(256–384)	512×256
Scan time	5:45	4:30

FSE fast spin-ech, MAVRIC multi-acquisition variable-resonance image combination, PDw proton density weighted

The MRI SI is proportional to the concentration of Gd-DTPA in the region and the native T1 relaxation time prior to injection of contrast. However, it is also affected by many tuning and scaling parameters even between series in the same imaging session [10, 31]. The normalization to cortical

bone was used to correct for minor variances in center frequency and transmit/receive gains between the pre- and post-contrast acquisitions. Cortical bone was chosen as a reference region, given the lack of signal available from free protons and the short T2 values [9, 19] This provided a region that would be minimally affected by enhancement from Gd-DTPA and therefore compensate for any changes in transmitter or receiver gain between scans.

Patients completed the short form 36 (SF-36) health survey, and the physical and mental component summaries were evaluated [35]. In addition, the patients were assessed using the Harris Hip Score (HSS) and each patient completed a visual analog scale (VAS) for pain at 12 months.

A  $\chi^2$  test was used to evaluate differences of detection rate of ON between MAVRIC and FSE images. A two-tailed Wilcoxon rank-sum test was performed to detect differences of measured ON volume between the FSE and MAVRIC acquisitions and differences of measured ON volume for each acquisition over time. A Friedman test was performed to detect differences of percent enhancement across the defined ROIs. Post hoc multiple comparison tests with Bonferroni corrections were performed when statistical significance was found. A *p* value of less than 0.05 was considered as statistically significant, with  $\alpha=0.05$ . Inter-reader

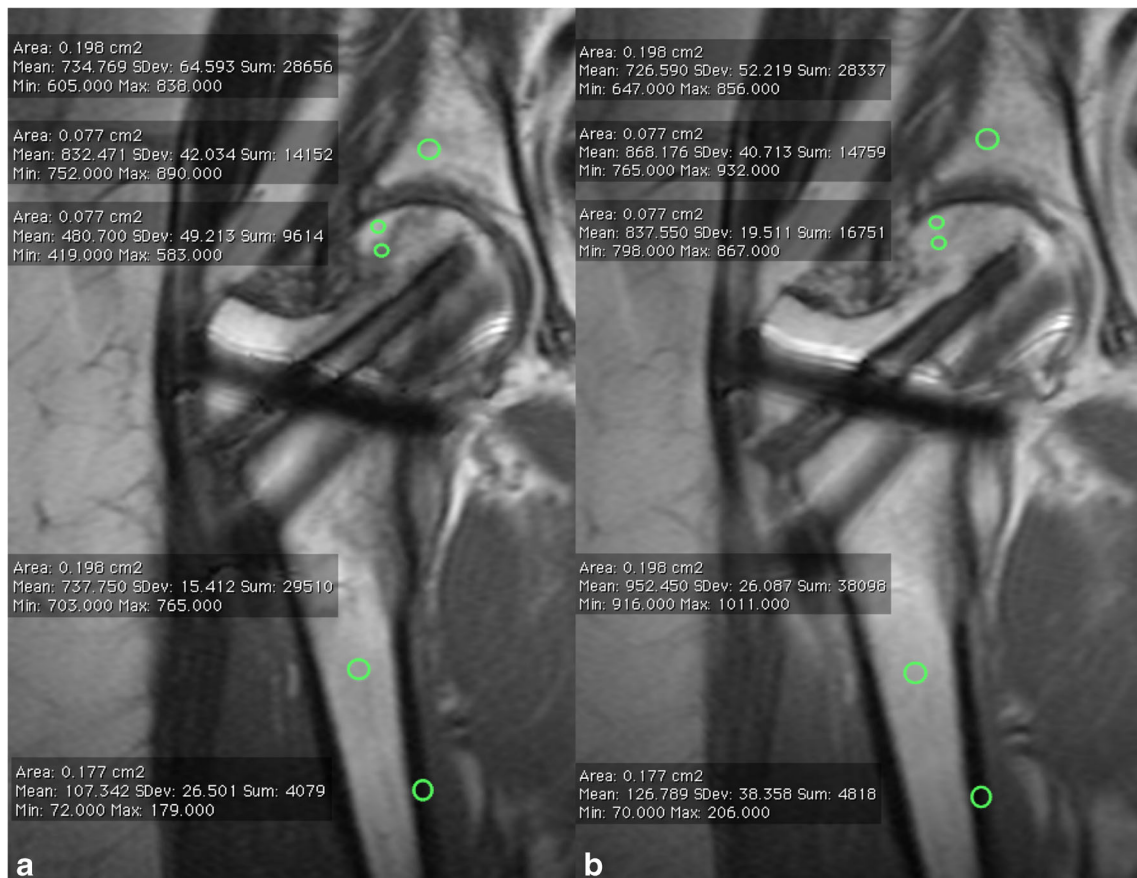


**Fig. 1.** A 63-year-old female with instrumentation of the proximal left femur for treatment of femoral neck fracture. **a** Pre- and **b** post-contrast coronal MAVRIC images show measurements of signal intensity enhancement with regions of interest (ROIs) placed within the center and within the rim of the osteonecrosis as well as within the ilium, femoral diaphysis, and cortex. The pre- and post-contrast images were linked together, ensuring that the ROIs were exactly the same size and at the exact same location for pre- and post-contrast measurements.

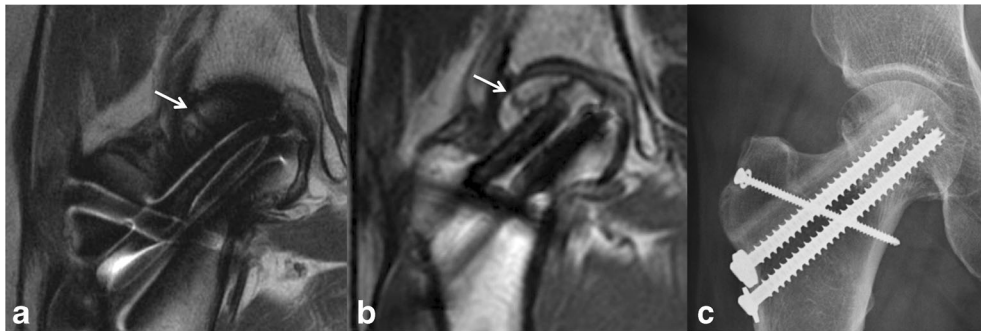


**Fig. 2.** A 71-year-old female with instrumentation of the proximal right femur for treatment of femoral neck fracture. Example of the detection of osteonecrosis (*arrows*) comparing **a** coronal 2D-FSE and **b** coronal MAVRIC sequences and **c** standard radiographs. The osteonecrosis on the 2D-FSE image is only partially detected (*arrow*), and its extent is underestimated as compared to the MAVRIC image (*arrow*) and is not discernible on the radiograph.

agreements between the two readers were accessed in a subset of patients ( $n=17$ ) at each time point using kappa statistics for the detection of ON, and the interclass correlation coefficient (ICC) for assessing SI enhancement. Spearman rank correlation of ON volume on FSE and MAVRIC scans with patient age, as well as ON volume change between 3 and 12 months on FSE and MAVRIC scans with patient age were performed, a Kruskal-Wallis test was performed to compare ON volume across the levels of Garden fracture classification, and a Wilcoxon rank-sum test was performed to compare ON volume between genders. Spearman rank correlations were also performed to evaluate the association between the presence and volume of ON at 12 months with the corresponding SF-36 survey, HSS, and VAS scores. Statistical analysis was performed using the SAS (SAS Institute, Cary, NC) software (V 9.3). In addition, a power analysis was performed for the ON-volume detection and SI enhancement [37].

## Results

Twenty-one consecutive patients were enrolled in the study. Four patients did not have a 12-month follow-up MRI exam. One of the four patients went on to total hip replacement because of fixation failure, and the remaining three patients withdrew from the study after their 3-month follow-up.

At 3 months postoperatively, ON was detected in 76% (16/21) of patients with pre-contrast MAVRIC images and in 67% (14/21) of patients with 2D-FSE images. At 12 months postoperatively, ON was detected in 77% (13/17) of patients with pre-contrast MAVRIC images and in 71% (12/17) of patients with 2D-FSE images. The ON detection rate was similar for images from each pulse sequence at for the combined time points,  $p=0.9214$ . ON was detected in 0% (0/21) of patients at 3 months and 6% (1/17) of patients at 12 months with conventional radiographs.

Representative FSE, MAVRIC, and radiographic images displaying the limited extent, full extent, and lack of ON within the femoral head, respectively, following FNF are shown in Fig. 2. In total, ON was detected in 29 of 38 cases (3 and 12 months combined). ON of three patients would have gone undetected using only

2D-FSE images at the 3- and 12-month follow-up exam. The inter-reader agreement for the detection of ON with FSE images was very good ( $\kappa=0.84$ ) and perfect when using MAVRIC images ( $\kappa=1$ ).

A significant difference in ON volume was detected at 3 months after surgery between the MAVRIC images ( $6.3 \text{ cm}^3 \pm 3.6 \text{ cm}^3$ ) and the FSE images ( $2.8 \text{ cm}^3 \pm 2.2 \text{ cm}^3$ ),  $p<0.0001$ . This difference was also found at 12 months after surgery ( $5.1 \text{ cm}^3 \pm 3.6 \text{ cm}^3$  [MAVRIC] versus  $2.1 \text{ cm}^3 \pm 1.4 \text{ cm}^3$ ;  $p=0.024$ ) (Fig. 3). No change in the volume of ON was detected over time, either for the FSE,  $p=1.0$ , or for MAVRIC,  $p=0.38$ . No significant correlations were found between ON volume or ON volume change with patient age,  $p \geq 0.13$ . No differences of ON volume by Garden fracture classification,  $p \geq 0.17$ , or between genders,  $p \geq 0.08$ , were detected.

Due to the decreased conspicuity of the ON segment on FSE images, the presence and degree of collapse was always more conspicuous on the MAVRIC images and used in the statistical analysis. Subchondral collapse was seen on MRI at 3 months in 14% (3/21) of patients with ON, which increased to 35% (6/17) after 12 months. Subchondral collapse was not seen on conventional

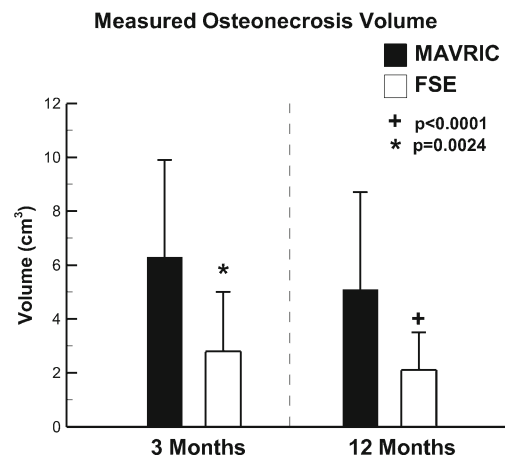


**Fig. 3.** Measured osteonecrosis volumes from FSE and MAVRIC images at 3 and 12 months postoperatively. *Bar graphs* are shown as mean  $\pm$  standard deviation.

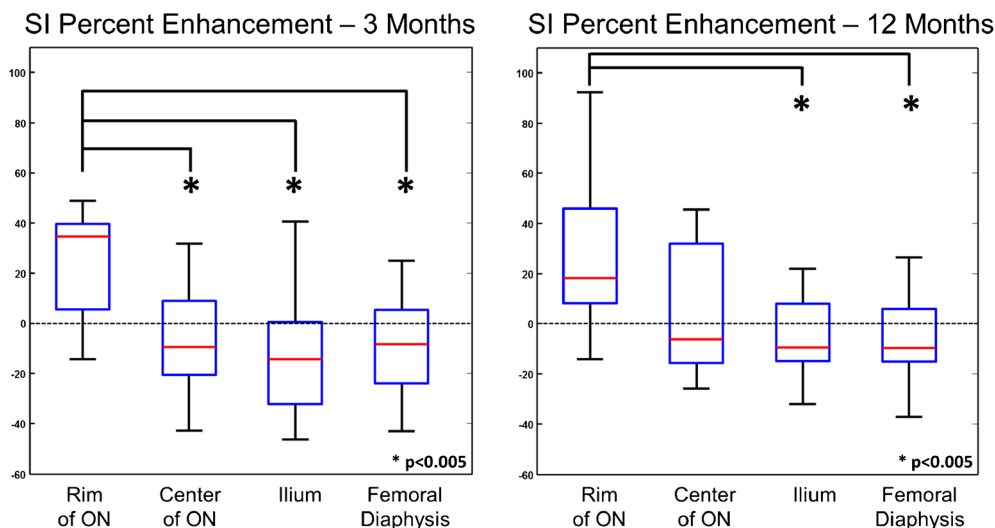


**Fig. 4.** Box plots of percentage SI enhancement of the osteonecrosis rim and osteonecrosis center compared to the ilium and femoral diaphysis at 3 and 12 months after surgery as assessed from MAVRIC images; all measurements were corrected for cortical bone. Note the significant increase in percentage signal intensity enhancement in the osteonecrosis rim compared to the ilium and femoral diaphysis. Box plots are depicted with whiskers from minimum to maximum, median and interquartile range.

radiographs at either time point. All cases of subchondral collapse disclosed only minimal loss of curvature of the subchondral bone; only one collapse measured 3 mm cortical depression and all others measured 2 mm or less.

There was a significantly higher percent SI enhancement in the rim of the ON ( $24\% \pm 22\%$ ) as compared to the center of the ON ( $-2\% \pm 28\%$ ), ilium ( $-14\% \pm 21\%$ ), and FD ( $-6\% \pm 27\%$ ) after 3 months (all  $p < 0.0035$ ) (Figs. 4 and 5). This finding was only maintained between the rim of the ON ( $29\% \pm 31\%$ ), ilium ( $-4\% \pm 16\%$ ), and FD ( $-7\% \pm 18\%$ ) after 12 months (all  $p < 0.005$ , Fig. 5). The contrast enhancement difference between the center of the ON lesion and the ilium or the femoral diaphysis was similar at 3 months ( $p = 0.09$

and  $p = 0.7$ ) and 12 months ( $p = 0.59$  and  $0.41$ ). There was no significant change in SI enhancement at 3 months versus 12 months for the rim and the center of the ON (both  $p = 1.0$ ). The inter-reader agreements for the SI enhancement were very good at 3 months ( $ICC = 0.79$ ) and at 12 months ( $ICC = 0.74$ ).

Patient-related outcome measures data was collected at  $13.9 \pm 8.0$  months following fracture fixation surgery. The patients had an average HHS of  $85.0 \pm 14.3$  and an average VAS of  $1.2 \pm 2.0$ . The physical component summary (PCS) and mental component summary (MCS) of the SF-36 were  $48.7 \pm 9.0$  and  $52.6 \pm 11.6$ , respectively. No significant correlations were found between these metrics and the corresponding presence and volume of ON at 12 months,  $p \geq 0.08$ .

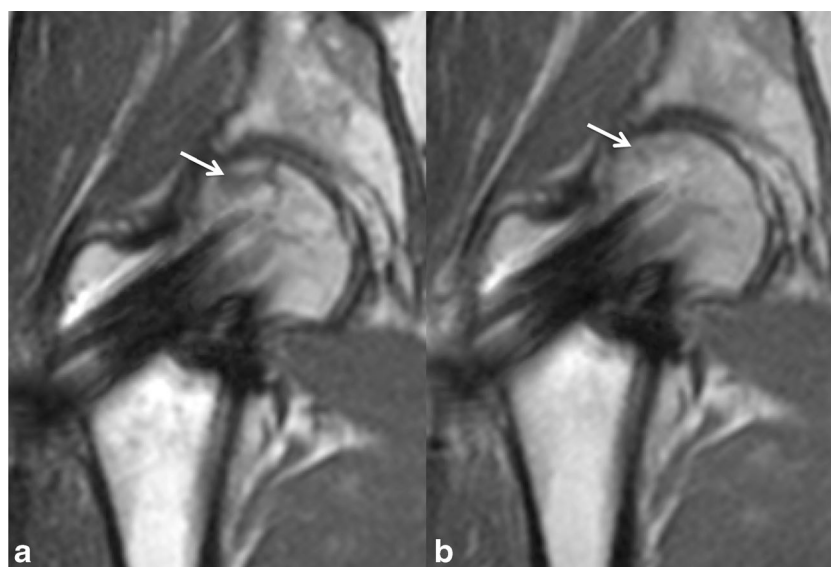


**Fig. 5.** A 53-year-old male with pin fixation for femoral neck fracture. **a** Pre- and **b** post-contrast coronal MAVRIC images show osteonecrosis with the ischemic-viable bone interface rim (arrow) in the **a** pre-contrast image and enhancement of the rim (arrow) in the **b** post-contrast image.

We performed a post hoc power analysis. We had a power of 0.8 for the detection of a 1.8-cm<sup>3</sup> difference of ON volume at 3 months (21 patients) and for the detection of a 1.86-cm<sup>3</sup> difference of ON volume at 12 months (17 patients). Similarly, we had a power of 0.8 for the detection of a 14.5% change in SI enhancement at 3 months (21 patients) and 12 months (17 patients).

## Discussion

This study assessed the detection rate and volume of ON around metallic implants after FNF, using standard 2D-FSE and MAVRIC imaging. In addition, semi-quantitative perfusion and post-contrast SI enhancement measurements were performed using MAVRIC. The results indicate that standardized radiographs underestimate the prevalence of ON after FNF fixation as compared to MRI, and 2D-FSE images underestimate the volume of the ON as compared to MAVRIC images. The study also demonstrates that an estimated semi-quantitative perfusion using the MAVRIC is feasible, and a significant increase in SI enhancement in the rim of the ON was detected.

The current study detected less than 10% of ON after internal fixation when using conventional radiographs. This result is comparable to results of previous reports that showed a prevalence of ON after internal fixation to be between 11 and 25% [1, 4, 16, 18, 27, 28]. A higher detection of ON at 3 months and at 12 months (77%) using of MRI is shown in the current study. While it seems plausible that this difference in observed prevalence of ON is most likely caused by the tomographic nature and superior soft tissue contrast of MRI, it must be noted that the majority of our patients had displaced FNF. A further explanation for the high underestimation using conventional radiographs after FNF fixation is due to the time frame of image acquisition. In general, ON is detected on conventional radiographs at a relatively late stage, in which bone changes are visible as a result of subchondral resorption or collapse [34]. Furthermore, the majority of the ON noted on MRI were located anterosuperiorly and were confined to the superficial subchondral region. The volume and extent of ON may be undetected on radiographs if the ON has a shallow depth on the femoral head and extends in the anterior-posterior direction. In this case, the ON would be seen across numerous coronal imaging planes using MRI but would be overlapped on an anterior-posterior radiograph displaying a limited area for ON subsequent detection. The current findings using MRI are in agreement with a previous study, which reported 47% of ON at 1-month follow-up with no changes in further follow-up images, despite collapse of the femoral head [32]. Even in the presence of ON, the patients in this cohort had HHS classified as “good” (range of 80–90) [12], and the PCS and MCS of the SF-36 scores indicated near normative physical and mental capacities.

An interesting finding is the lack of difference in the detection rate of ON between 2D-FSE and MAVRIC but the measured volume of ON was higher using MAVRIC images.

When using an FSE sequence optimized for imaging around metallic hardware by use of a wide receiver bandwidth, ON could be detected in a small region of the femoral head; however, evaluating the full extent of ON was limited due to magnetic susceptibility artifact. MAVRIC provided superior image quality near the stainless steel fixation hardware, as previously reported [13], and permitted greater visualization of the extent of ON. We do not attribute the larger volume of ON measured using MAVRIC to enlargement caused by artifacts since MAVRIC minimizes both in-plane and through-plane distortions relative to known dimensions in the presence of metal [22], and it is unclear at the present time how patient treatment may be affected by knowledge of the full extent of ON. Finally, the ON was located primarily in the supero-medial quadrant in the same patient cohort by Dyke et al. [6] and correlates very well with the preoperatively measured hypoperfusion in the supero-medial quadrant using LAVA-perfusion measurements [6].

Dynamic MRI was recently introduced to study femoral head viability after FNF, but follow-up studies have been limited to conventional radiographs, potentially resulting in a high false-negative detection rate for ON [18]. A quantitative perfusion evaluation using pre- and postoperative SI measurements from MAVRIC images was introduced in this study. Perfusion measurements frequently use gradient recalled echo (GRE) sequences for data acquisition, but these sequences would be severely degraded due to the presence of magnetic susceptibility in the setting of stainless steel hardware. MAVRIC was required to determine the percentage increase of SI due to its ability to reduce in-plane and suppress through-plane artifact near the implanted hardware. The results showed a large percentage SI enhancement at the interface of the ON and at the surrounding normal bone marrow at 3 and 12 months postoperatively. This increase in uptake may be attributable to vascular regeneration and reparative tissue in the transitional zone, as already described in previous literature [7, 23, 30].

There are several limitations to the current study. First, the number of patients enrolled in the study was not very large, but the power analysis found sufficient power for a majority of the statistical analyses performed. Therefore, the number of patients enrolled in the study was sufficient for statistical purposes. It is challenging to enroll a large number of patients who have a displaced femoral neck fracture, who underwent surgical screw fixation (instead of hip prosthesis), and who agree to be followed by MRI examinations after 3 and 12 months. We believe the results of this study may be used with confidence in assessing patients with ON but caution that the study only evaluated patient for 1 year postoperatively and that longer follow-up evaluation may be necessary. It is unclear how the presence and extent of ON at this time point may affect clinical outcome. In addition, future studies with greater patient enrollment may be able to evaluate the correlations between the metrics of ON volume with patient age, differences of ON volume by level of Garden fracture classification, as well as the effects of gender.

Second, the detection and the volume of FSE versus MAVRIC were compared using PD FSE and MAVRIC images. The presence of ON was determined based on definitive recognition of the ischemic-viable bone interface, rather than differences of signal intensity alone. Since the detection rate of ON did not significantly differ between the unenhanced MAVRIC and the PD FSE sequences, we believe it is feasible to compare the two sequences. Third, only MRI was used to assess the presence and volume of ON. Although computerized tomography (CT) may also be used for ON detection, MRI has been shown to be the most accurate imaging modality used for the diagnosis of ON in the femoral head due to its direct multi-planar capabilities and superior soft tissue contrast [24]. Fourth, no comparison between MRI and corresponding pathology or surgical assessment of vascularity of the bony anatomy was available for the current cohort [5]. Finally, the current cohort may not be representative of all patients presenting with FNF, as most of the patients in this study had displaced FNF. The prevalence of ON may be different in patients with non-displaced FNF, who may not require surgical fixation of their fracture.

In conclusion, conventional radiographs underestimate ON after internal FNF fixation, and MAVRIC is superior to 2D-FSE imaging for quantifying the extent of ON around metallic implants. In addition, quantitative perfusion measurements with post-contrast SI enhancement measurements using the MAVRIC sequence are feasible to provide an indirect assessment of perfusion. Future longitudinal studies with larger cohorts may provide important prediction modeling for the risk of collapse and the development of osteoarthritis, as well as the need to perform such screening procedures for ON in asymptomatic cohorts following instrumentation for treatment of displaced FNF.

**Acknowledgments** The authors would like to thank Joo Jung RT (MR) for his assistance in performing this study. This project has been supported by a grant from the AO Research Fund of the AO Foundation (AO Research Grant F-09-6H).

#### Disclosures

**Conflict of Interest:** Jonathan P. Dyke, PhD, Lionel E. Lazaro, MD, Parina Shah, MS and Dean G. Lorich, MD have declared that they have no conflict of interest. Nadja A. Farshad-Amacker, MD reports grants from AO Research Fund during the study. Matthew F. Koff, PhD reports other from GE Healthcare during the study. Hollis G. Potter, MD reports other from GE Healthcare during the study.

**Human/Animal Rights:** All procedures followed were in accordance with the ethical standards of the responsible committee on human experimentation (institutional and national) and with the Helsinki Declaration of 1975, as revised in 2008 (5).

**Informed Consent:** Informed consent was obtained from all patients for being included in the study.

**Required Author Forms** Disclosure forms provided by the authors are available with the online version of this article.

#### References

1. Ai ZS, Gao YS, Sun Y, Liu Y, Zhang CQ, Jiang CH. Logistic regression analysis of factors associated with avascular necrosis of the femoral head following femoral neck fractures in middle-aged and elderly patients. *J Orthop Sci.* 2013; 18(2): 271-276.
2. Arnoldi CC, Lemperg RK. Fracture of the femoral neck. II. Relative importance of primary vascular damage and surgical procedure for the development of necrosis of the femoral head. *Clin Orthop Relat Res.* 1977; 129(129): 217-222.
3. Bassett LW, Gold RH, Reicher M, Bennett LR, Tooke SM. Magnetic resonance imaging in the early diagnosis of ischemic necrosis of the femoral head. Preliminary results. *Clin Orthop Relat Res.* 1987; 214: 237-248.
4. Cobb AG, Gibson PH. Screw fixation of subcapital fractures of the femur—a better method of treatment? *Injury.* 1986; 17(4): 259-264.
5. Donati OF, Zanetti M, Nagy L, Bode B, Schweizer A, Pfirrmann CW. Is dynamic gadolinium enhancement needed in MR imaging for the preoperative assessment of scaphoidal viability in patients with scaphoid nonunion? *Radiology.* 2011; 260(3): 808-816.
6. Dyke JP, Lazaro LE, Hettrich CM, Hentel KD, Helfet DL, Lorich DG. Regional analysis of femoral head perfusion following displaced fractures of the femoral neck. *J Magn Reson Imaging.* 2013; 41(2): 550-554.
7. Ehlinger M, Moser T, Adam P, et al. Early prediction of femoral head avascular necrosis following neck fracture. *Orthop Traumatol Surg Res.* 2011; 97(1): 79-88.
8. Garden RS. Stability and Union in Subcapital Fractures of the Femur. *J Bone Joint Surg Br.* 1964; 46: 630-647.
9. Gatehouse PD, Bydder GM. Magnetic resonance imaging of short T2 components in tissue. *Clin Radiol.* 2003; 58(1): 1-19.
10. Gribbestad IS, Gjesdal KI, Nilsen G, Lundgren S, Hjelsteun MHB, Jackson A. *An Introduction to Dynamic Contrast-Enhanced MRI in Oncology. Medical Radiology.* Berlin/Heidelberg: Springer; 2005.
11. Gullberg B, Johnell O, Kanis JA. World-wide projections for hip fracture. *Osteoporos Int.* 1997; 7(5): 407-413.
12. Harris WH. Traumatic arthritis of the hip after dislocation and acetabular fractures: treatment by mold arthroplasty. An end-result study using a new method of result evaluation. *J Bone Joint Surg Am.* 1969; 51(4): 737-755.
13. Hayter CL, Koff MF, Shah P, Koch KM, Miller TT, Potter HG. MRI after arthroplasty: comparison of MAVRIC and conventional fast spin-echo techniques. *Am J Roentgenol.* 2011; 197(3): W405-W411.
14. Hayter CL, Koff MF, Potter HG. Magnetic resonance imaging of the postoperative hip. *J Magn Reson Imaging.* 2012; 35(5): 1013-1025.
15. Hernigou P, Poignard A, Nogier A, Manicom O. Fate of very small asymptomatic stage-I osteonecrotic lesions of the hip. *J Bone Joint Surg Am.* 2004; 86-A(12): 2589-2593.
16. Jakob M, Rosso R, Weller K, Babst R, Regazzoni P. Avascular necrosis of the femoral head after open reduction and internal fixation of femoral neck fractures: an inevitable complication? *Swiss Surg.* 1999; 5(6): 257-264.
17. Kannus P, Parkkari J, Sievanen H, Heinonen A, Vuori I, Jarvinen M. Epidemiology of hip fractures. *Bone.* 1996; 18(1 Suppl): 57S-63S.
18. Kaushik A, Sankaran B, Varghese M. To study the role of dynamic magnetic resonance imaging in assessing the femoral head vascularity in intracapsular femoral neck fractures. *Eur J Radiol.* 2010; 75(3): 364-375.
19. Khurana JS. *Bone Pathology.* 2nd ed. New York: Humana Press; 2009.
20. Koch KM, Hargreaves BA, Pauly KB, Chen W, Gold GE, King KF. Magnetic resonance imaging near metal implants. *J Magn Reson Imaging.* 2010; 32(4): 773-787.
21. Koch KM, Brau AC, Chen W, et al. Imaging near metal with a MAVRIC-SEMAC hybrid. *Magn Reson Med.* 2011; 65(1): 71-82.

22. Koff MF, Shah P, Koch KM, Potter HG. Quantifying image distortion of orthopedic materials in magnetic resonance imaging. *J Magn Reson Imaging*. 2013; 38(3): 1083-1091.
23. Lang P, Jergesen HE, Moseley ME, Block JE, Chafetz NI, Genant HK. Avascular necrosis of the femoral head: high-field-strength MR imaging with histologic correlation. *Radiology*. 1988; 169(2): 517-524.
24. Lavernia CJ, Sierra RJ, Grieco FR. Osteonecrosis of the femoral head. *J Am Acad Orthop Surg*. 1999; 7(4): 250-261.
25. Lieberman JR, Berry DJ, Mont MA, et al. Osteonecrosis of the hip: management in the 21st century. *Instr Course Lect*. 2003; 52: 337-355.
26. Lofthus CM, Osnes EK, Falch JA, et al. Epidemiology of hip fractures in Oslo. *Norway Bone*. 2001; 29(5): 413-418.
27. Lu-Yao GL, Keller RB, Littenberg B, Wennberg JE. Outcomes after displaced fractures of the femoral neck. A meta-analysis of one hundred and six published reports. *J Bone Joint Surg Am*. 1994; 76(1): 15-25.
28. Min BW, Kim SJ. Avascular necrosis of the femoral head after osteosynthesis of femoral neck fracture. *Orthopedics*. 2011; 34(5): 349.
29. Nikolopoulos KE, Papadakis SA, Kateros KT, et al. Long-term outcome of patients with avascular necrosis, after internal fixation of femoral neck fractures. *Injury*. 2003; 34(7): 525-528.
30. Sakai T, Sugano N, Nishii T, Haraguchi K, Ochi T, Ohzono K. MR findings of necrotic lesions and the extralesional area of osteonecrosis of the femoral head. *Skeletal Radiol*. 2000; 29(3): 133-141.
31. Sansone M, Aprile F, Fusco R, Petrillo M, Petrillo A, Siani A et al. A study on reference based time intensity curves quantification in DCE-MRI monitoring of rectal cancer. World Congress on Medical Physics and Biomedical Engineering; Sept 7-12; Munich, Germany: IFMBE Proceedings; 2009: 38-41.
32. Sugano N, Masuhara K, Nakamura N, Ochi T, Hirooka A, Hayami Y. MRI of early osteonecrosis of the femoral head after transcervical fracture. *J Bone Joint Surg Br*. 1996; 78(2): 253-257.
33. Takatori Y, Kokubo T, Ninomiya S, Nakamura S, Morimoto S, Kusaba I. Avascular necrosis of the femoral head. Natural history and magnetic resonance imaging. *J Bone Joint Surg Br*. 1993; 75(2): 217-221.
34. Totty WG, Murphy WA, Ganz WI, Kumar B, Daum WJ, Siegel BA. Magnetic resonance imaging of the normal and ischemic femoral head. *AJR Am J Roentgenol*. 1984; 143(6): 1273-1280. doi:10.2214/ajr.143.6.1273.
35. Ware JE Jr, Sherbourne CD. The MOS 36-item short-form health survey (SF-36). I. Conceptual framework and item selection. *Med Care*. 1992; 30(6): 473-483.
36. Zalavras CG, Lieberman JR. Osteonecrosis of the femoral head: evaluation and treatment. *J Am Acad Orthop Surg*. 2014; 22(7): 455-464.
37. Zar JH. *Biostatistical Analysis*. Englewood Cliffs: Prentice Hall; 1984.